Acoustic instability prediction via an impedance criterion

Application to the flow through a circular aperture in a thick plate

Javier Sierra[1,2], D. Fabre[1], F. Giannetti[2], V. Citro[2]

[1] UPS-IMFT, Institut de Mécanique des fluides de Toulouse, Toulouse 31400, France
[2] UNISA, Universitá degli Studi di Salerno,Fisciano 84084, Italy

Table of contents

Flow configuration

Flow configuration

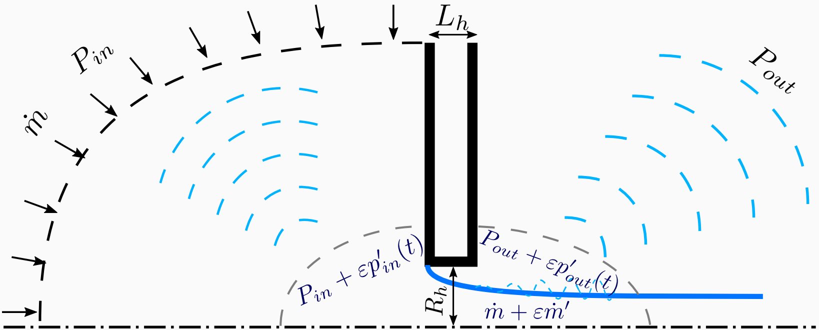

Figure 1: Sketch of the open/open configuration. Whistle Category II (Chanaud 1970)

$$Re = \frac{\rho_0 D_h U_M}{\mu} \equiv \frac{2\dot{m}_0}{\pi R_h \mu}; \quad M = \frac{U_M}{c_0} \text{ with } c_0 = \sqrt{\gamma R_g T_0}; \qquad (1)$$
$$\beta = \frac{L_h}{2R_h} = \frac{L_h}{D_h}$$

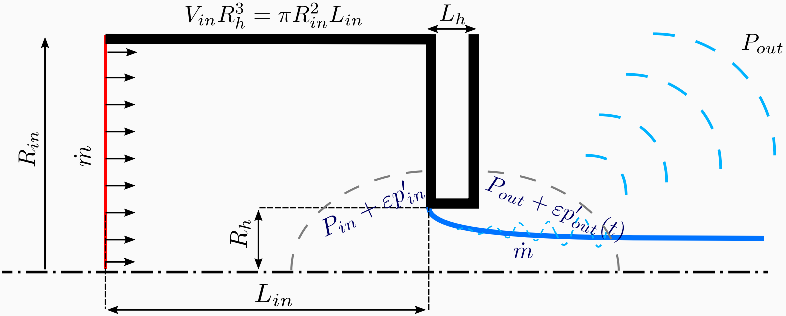

Figure 2: Sketch of the closed/open configuration. Whistle Category III (Chanaud 1970)

$$V_{in} = \frac{L_{in}\pi R_{in}^2}{R_h^3}. \tag{2}$$

Governing equations

Let consider a compressible fluid motion of a perfect gas described in primitive variables by $\mathbf{q} = [\rho, \mathbf{u}, T, p]^T$, where the velocity vector field is $\mathbf{u} = (u, v, w)$, pressure p, temperature T and fluid density ρ. Dimensional primitive variables have been made dimensionless as follows:

$$\mathbf{x} = \frac{\tilde{\mathbf{x}}}{D_h}, \quad t = \frac{\tilde{t} U_M}{D_h}, \quad \rho = \frac{\tilde{\rho}}{\rho_0}, \quad \mathbf{u} = \frac{\tilde{\mathbf{u}}}{U_M}, \quad T = \frac{\tilde{T}}{T_0}, \quad p = \frac{\tilde{p} - p_0}{\rho_0 U_M^2} \tag{3}$$

$$\mathbf{M}\left(\frac{\partial \mathbf{q}}{\partial t}\right) = \mathcal{NS}(\mathbf{q}) = \mathbf{L}(\mathbf{q}) + \mathbf{N}(\mathbf{q}) + \mathbf{C} = \mathbf{0} \tag{4}$$

Methodology

Governing equations (II)

$$\mathsf{M}(\frac{\partial \mathbf{q}}{\partial t}) = \mathcal{NS}(\mathbf{q}) = \mathsf{L}(\mathbf{q}) + \mathsf{N}(\mathbf{q}) + \mathsf{C} = \mathbf{0} \tag{5}$$

where $\mathsf{C} = [0, \mathbf{0}, 0, 1]^T$, the mass matrix, the linear operator are as follows:

$$\mathsf{M} = \begin{pmatrix} 1 & 0 & 0 & 0 \\ 0 & \rho\mathbf{I} & 0 & 0 \\ 0 & 0 & \rho & 0 \\ 0 & 0 & 0 & 0 \end{pmatrix}, \quad \mathsf{L} = \begin{pmatrix} 0 & 0 & 0 & 0 \\ 0 & -\nabla\cdot\tau(\cdot) & 0 & \nabla \\ 0 & 0 & -\frac{\gamma}{PrRe}\Delta & 0 \\ 0 & 0 & 0 & \gamma M^2 \end{pmatrix} \tag{6}$$

and the nonlinear operator is written as:

$$\mathsf{N}(\mathbf{q}) = \begin{pmatrix} \mathbf{u}\cdot\nabla\rho + \rho\nabla\cdot\mathbf{u} \\ \rho\mathbf{u}\cdot\nabla\mathbf{u} \\ (\gamma-1)\Big[\rho T\nabla\cdot\mathbf{u} - \gamma M^2\tau(\mathbf{u}) : \mathsf{D}(\mathbf{u})\Big] + \rho\mathbf{u}\cdot\nabla T \\ -\rho T \end{pmatrix}, \tag{7}$$

$$\mathcal{NS}\left(\mathbf{q}_0\right) = \mathsf{L}\left(\mathbf{q}_0\right) + \mathsf{N}(\mathbf{q}_0) + \mathsf{C} = \mathbf{0} \tag{8}$$

with boundary conditions

$$\int_{\Gamma_{in}} \rho_0 \mathbf{u_0} \cdot \mathbf{n} dS = \dot{m}_0 \tag{9a}$$

$$p_0 = P_{in} \quad \text{on} \quad \Gamma_{in}, \tag{9b}$$

$$p_0 = P_{out} \quad \text{on} \quad \Gamma_{out}. \tag{9c}$$

Flow stability (II) – Gen. eigenvalue problem

The evolution of the perturbation $\hat{\mathbf{q}}$, where

$$\mathbf{q}(t) = \mathbf{q}_0 + \varepsilon\left(\hat{\mathbf{q}}e^{-i\omega t} + \text{c.c.}\right) \tag{10}$$

is governed by the linearised compressible Navier–Stokes equations

$$-i\omega \mathsf{M}\hat{\mathbf{q}} = \mathcal{LNS}_0\left(\hat{\mathbf{q}}\right) = \left[\mathsf{L} + D\mathsf{N}\big|_{\mathbf{q}_0}\right]\hat{\mathbf{q}}, \tag{11}$$

- With the purpose of modelling a large container upstream of the hole the Complex Mapping technique [5]; it is set both upstream and downstream, to avoid any nonphysical reflection into the domain of interest. At the far-field constant density equal to ρ_0 is set and stress-free boundary condition.
- For the purpose of modelling a closed cavity that acts as an acoustic resonator, no-slip boundary conditions are set at the inlet with constant density ρ_0; stress-free condition and constant density ρ_0 is set at the outlet. In this case, we used a complex mapping in the region downstream of the hole.

Flow stability (III) – Impedance criterion

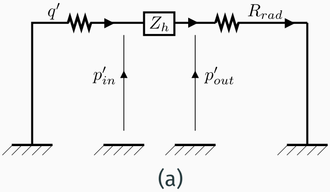

Figure 3: Sketch of the electric analogy of the model employed for *open/open* (a) and for the *cavity/open* (b) configurations.

Hypothesis: Mach number is small and coustic wavelengths are much larger than the dimensions of the hole (**acoustic compactness hypotheses**).

$$p_{in}(t) = P_{in} + p'_{in} e^{-i\tilde{\omega}t}, \quad p_{out}(t) = P_{out} + p'_{out} e^{-i\tilde{\omega}t},$$
$$q(t) = Q_0 + q' e^{-i\tilde{\omega}t},. \tag{12}$$

Impedance modelling (I)

- Inner region : hole impedance

$$Z_h(\omega) = \left[\frac{R_h^2}{\rho_0 U_M}\right] \frac{p'_{in} - p'_{out}}{q'} \tag{13}$$

- Downstream (resp. upstream in open configuration) region : radiation impedance

$$Z_{rad} = \left[\frac{R_h^2}{\rho_0 U_M}\right] \frac{p'_{out}}{q'} = \frac{M\omega^2}{2\pi} \tag{14}$$

- Upstream region : case of a closed domain

$$Z_{cav} = \left[\frac{R_h^2}{\rho_0 U_M}\right] \frac{p'_{in}}{q'} = \frac{i}{\omega M^2 V_{in}} = \frac{i}{\omega \chi}, \quad \chi = M^2 V_{in} \tag{15}$$

Impedance modelling (II)

Regrouping all regions, we are able to obtain a single constitutive equation allowing to determine the eigenfrequencies of the problem, featuring a *total impedance* of the full system, noted either Z_a or Z_b for the two investigated configurations:

(a): For the open/open configuration, $Z_h = -2Z_{rad}$, or equivalently :

$$Z_a(\omega) = Z_h(\omega) + \frac{M\omega^2}{\pi} = 0 \tag{16}$$

(b): for the cavity/open configuration, $Z_h = -Z_{cav} - Z_{rad}$, or equivalently :

$$Z_b(\omega) = Z_h(\omega) + \frac{M\omega^2}{2\pi} + \frac{i}{M^2 V_{in}\omega} = 0 \tag{17}$$

Impedance modelling (III)

Following an idea previously used in [4], we will assume that the impedance of the full system is mostly reactive. We first elaborate this idea for the cavity/open configuration. The hypotheses are as follows:

1. $\omega = \omega_0 + \omega_1, \quad \omega_0 \in \mathbb{R}, \quad \omega_1 \in \mathbb{C}, \quad , |\omega_1| \ll |\omega_0|,$
2. $|\mathrm{Re}(Z_h)| \ll |\mathrm{Im}(Z_h)|$
3. $\frac{M\omega^2}{2\pi} \ll |\mathrm{Im}(Z_h)|$

The conditions for instability are $Z_a = 0$ and $Z_b = 0$.

Look for it performing a Taylor development in terms of the assumed small quantities leads to

$$\begin{aligned} Z_b(\omega) = \quad & i\Big[Z_{h,I}(\omega_0) + \frac{1}{M^2 V_{in}\omega_0}\Big] \\ & + \Big[Z_{h,R}(\omega_0) + \tfrac{M\omega_0^2}{2\pi} + \Big(\big(\tfrac{\partial Z_h}{\partial \omega}\big)_{\omega=\omega_0} - \tfrac{i}{M^2 V_{in}\omega_0^2}\Big)\omega_1\Big] \\ & + h.o.t. \end{aligned} \tag{18}$$

Impedance modelling (IV)

- Closed domain (Z_b)
  1. The 0^{th}-order terms lead to the condition
$$-\omega_0 Z_{h,I}(\omega_0) = \frac{1}{M^2 V_{in}} = \frac{1}{\chi} \tag{19}$$
  2. Secondly, the first-order term leads to
$$\omega_1 = \frac{-\left[Z_{h,R}(\omega_0) + \frac{M\omega_0^2}{2\pi}\right]}{\left(\frac{\partial Z}{\partial \omega}\right)_{\omega=\omega_0}} \tag{20}$$
- Open domain (Z_a)
  1. The 0^{th}-order terms lead to the condition
$$-\omega_0 Z_{h,I}(\omega_0) = 0 \tag{21}$$
  2. Secondly, the first-order term leads to
$$\omega_1 = \frac{-Z_{h,R}(\omega_0)}{\left(\frac{\partial Z_h}{\partial \omega}\right)_{\omega=\omega_0}} = \frac{-\left[Z_{h,R}(\omega_0) + \frac{M\omega_0^2}{\pi}\right]}{\left(\frac{\partial Z_h}{\partial \omega}\right)_{\omega=\omega_0}} \tag{22}$$

Impedance modelling (V)

- A *direct method*
  1. Given the parameters M and V_{in} determine ω_0 as an *implicit* function of χ (as sketched in figure 5a).
  2. Then ω_1 is an *explicit* function of ω_0 and M.
  3. $\omega = \omega_0 + \omega_1$, unstable if $Im(\omega_1) > 0$

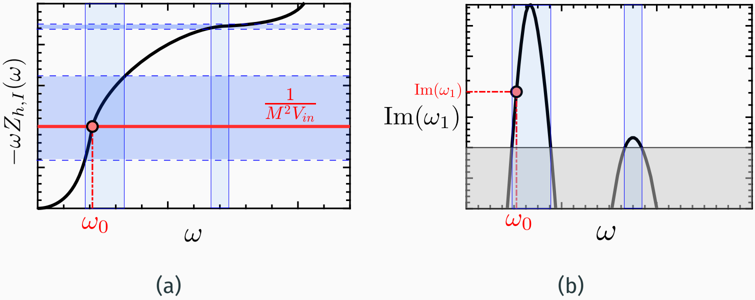

Figure 4: Zeroth-order (a) and first order (b)

Impedance modelling (VI)

- *Inverse method.*
    1. M is given, determine $Im(\omega_1)$ as a function of ω_0 and deduce the ranges of ω_0 where this function is positive (as indicated in blue on figure 5*b*).
    2. Deduce the corresponding ranges for $1/(M^2 V_{in})$ from 0^{th} order correction.
    3. The approach will thus indicate the ranges of V_{in} where, for the given M, the jet is unstable.

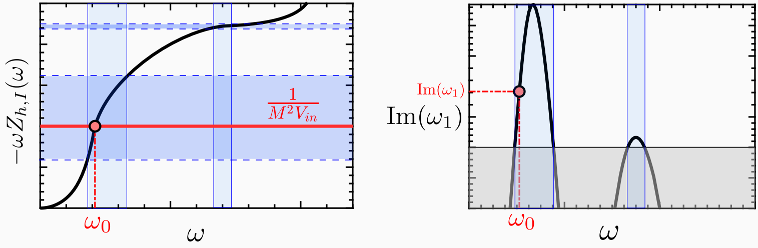

(a) (b)

Results

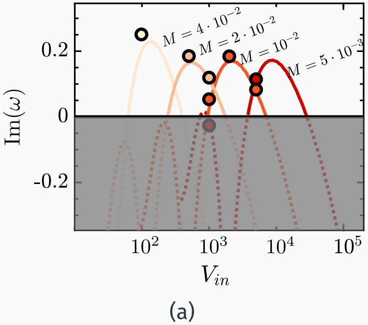

Figure 6: Lines were obtained from the asymptotically matched model and points with compressible LNSE. Solid lines denote unstable regions, dashed lines are used for stable zones. $Re = 1600$.

Stability criterion for the closed domain ($Re - \chi$)

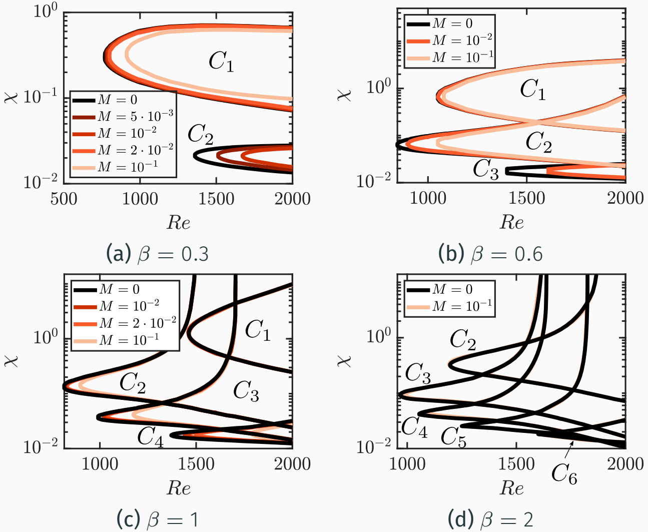

Figure 7: Regions of conditional stability in the (χ, Re) plane.

Stability criterion for the closed domain ($M - V_{in}$)

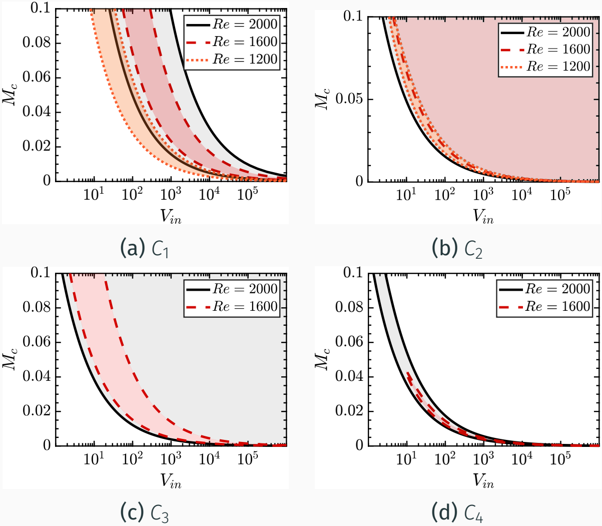

(a) C_1 (b) C_2

(c) C_3 (d) C_4

Figure 8: Regions of conditional stability in the (V_{in}, M) plane for $\beta = 1$.

A word about the open-configuration

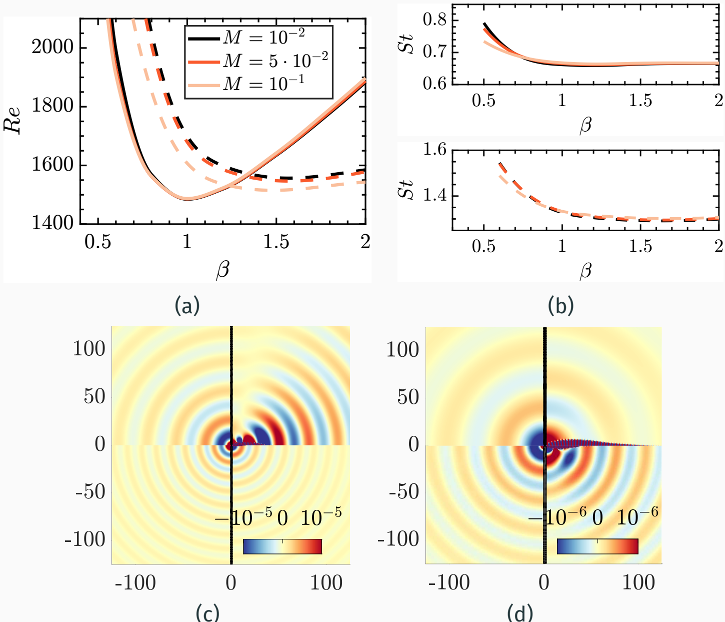

(a) (b)

(c) (d)

Conclusion

Summary

- Study of the stability of the acoustic flow field past a thick hole.
- Modelling of the configuration in terms of a scalar transfer function: *impedance*.
- Simplified instability criterion in terms of the *impedance*. Faster parametric analysis than linearised compressible Navier–Stokes.
- Good matching as long as the sources are acoustically compact.

Codes for compressible steady-state, compressible linearised and incompressible forced problems are available in

https://gitlab.com/stabfem/StabFem

For more details, [1, 2, 3]

Questions?

D. Fabre, V. Citro, D. Ferreira Sabino, P. Bonnefis, J. Sierra, F. Giannetti, and M. Pigou.
A practical review on linear and nonlinear global approaches to flow instabilities.
Applied Mechanics Reviews, 70(6), 2018.

D. Fabre, R. Longobardi, P. Bonnefis, and P. Luchini.
The acoustic impedance of a laminar viscous jet through a thin circular aperture.
Journal of Fluid Mechanics, 864:5–44, 2019.

D. Fabre, R. Longobardi, V. Citro, and P. Luchini.
Acoustic impedance and hydrodynamic instability of the flow through a circular aperture in a thick plate.
Journal of Fluid Mechanics, 885, 2020.

References ii

D. Ferreira Sabino, D. Fabre, J. Leontini, and D. Lo Jacono.
Vortex-induced vibration prediction via an impedance criterion.
Journal of Fluid Mechanics, 890(A4):1–22, 2020.

J. Sierra, D. Fabre, and V. Citro.
Efficient stability analysis of fluid flows using complex mapping techniques.
Computer Physics Communications, 251:107100, 2020.